

# Growth and characterization of glycinium oxalate crystals for nonlinear optical applications

K. J. ARUN\*, S. JAYALEKSHMI

*Division for research in advanced materials, Department of Physics, Cochin University of Science and Technology, Kochi-682022, Kerala, India*

Single crystals of Glycinium oxalate (GLO) are grown by top seeded solution growth method. Characterization of the grown crystal is done by CHN test and powder X-ray diffraction. UV-Vis-NIR, FTIR spectroscopic analysis, thermal studies by TGA/ DTA and DSC, photoconductivity and photoluminescence studies, micro topography and chemical etching studies have also been carried out. crystal has a wide transparency window from 324nm to 2500 nm making it suitable for applications in the whole region for higher harmonic generation and other optoelectronic applications. The good thermal stability of the material ensures its suitability for possible applications in lasers, where the crystals are required to withstand high temperatures. Z scan study under open aperture configuration illustrates the nonlinear optical behaviour of the grown crystal. The comparatively high value of two photon absorptive index demonstrates that the GLO crystal has potential for optical limiting applications.

(Received September 28, 2008; accepted October 6, 2008)

*Keywords:* Crystal growth, Nonlinear optics, Thermal studies, Photoconductivity

## 1. Introduction

In recent years, one has witnessed increasing interest in the study of amino acids and their derivative crystals. This interest has been stimulated by the perspective of understanding a system where the hydrogen bonding plays a fundamental role and, as a result of this understanding, a better knowledge of some important biological molecules can be achieved. Amino acid crystals with delocalized  $\pi$  electrons usually display large nonlinear optical (NLO) response and are potential candidates for applications in the emerging areas of photonics [1]. Most of such crystals are composed of dipolar aromatic molecules, which exhibit intramolecular charge transfer. Molecules that show asymmetric polarization induced by electron donor and acceptor groups in  $\pi$  electron conjugated molecules are responsible for electro optic and NLO properties [2].

The charge transfer complex of glycine and oxalic acid-glycinium oxalate (GLO), crystallizes in the monoclinic, non-centro symmetric space group P21/c with four formula units in the unit cell with  $a = 10.580\text{\AA}$ ,  $b = 5.650\text{\AA}$ ,  $c = 12.093\text{\AA}$ ,  $\alpha = \gamma = 90^\circ$ ,  $\beta = 113.83^\circ$ . It is an interesting non-linear optical material (NLO) because of the presence of excess of delocalized  $\pi$  electrons [3]. In the present investigation, growth aspects of GLO are studied and bulk crystals are grown by top seeded slow evaporation technique. Grown crystals are characterized by powder XRD, CHN test, TGA/ DTA, differential scanning calorimetry, micro topography and chemical etching studies, FTIR and UV-Vis-NIR spectroscopy, and photoconductivity and photo-luminescence studies. Open aperture Z scan technique is used to establish the NLO behaviour of the crystal.

## 2. Experimental

### 2.1 Synthesis and crystal growth

Glycinium oxalate (GLO) is synthesized from aqueous solutions of glycine and oxalic acid taken in 1:1 molar ratio. Seed crystals prepared using the synthesized powder are top seeded in its saturated solution at 280C, which yields good optical quality crystals in three weeks time (Fig. 1), with an optimum size of 10mm×10mm×3mm.

### 2.2 Characterization

Glycinium oxalate crystals are characterized by powder XRD, CHN test, Fourier transform infrared spectroscopy (FTIR), UV-Vis-NIR spectral analysis, microstructure studies using optical microscope, photoconductivity and photoluminescence studies. Nonlinear absorption coefficient is determined using Z scan technique.

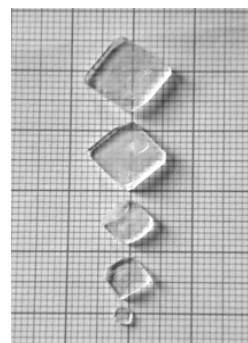


*Fig. 1. Glycinium oxalate crystals.*

### 3. Results and discussion

#### 3.1 CHN analysis

The chemical composition of the grown GLO crystal determined by carbon, hydrogen, nitrogen (CHN) analysis using VarioEL III CHNS serial number 11035060 is compared with the theoretical values of carbon, hydrogen and nitrogen present in the crystal and is shown in Table 1. From the results, the composition of the material is established as  $C_4H_7NO_2$ .

Table 1. CHN analysis data.

Element	Theoretical composition (%)	Measured composition (%)
Carbon	29.07	28.72
Hydrogen	4.24	4.42
Nitrogen	8.48	8.50

#### 3.2 X-ray powder diffraction

The powder X-ray diffractogram of the GLO crystal shown in the Fig. 2 is registered with Bruker D8 advance diffractometer operated at 40 KV and 50mA, using Cu target and graphite monochromator. The intensity data is recorded by continuous scan from  $5^\circ$  to  $60^\circ$  with a step size of  $0.02^\circ$  and scan speed of  $4^\circ/\text{minute}$ . The structure, refined by Pawley method [4] using the TOPAZ R version 3 program is given in table 2, which agrees well with the reported values [3].

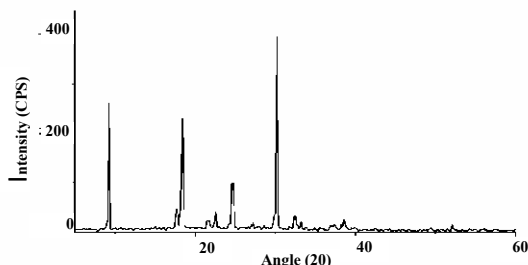


Fig.2. Powder X-ray diffractogram of GLO.

Table 2. Structure analysis data.

R-Bragg	33.632
Space group	P21/c
Cry.SizeLorentzian(nm)	200.2
k:1LVol-IB(nm)	127.446
k:0.89 LVol-FWHM (nm)	178.171
Strain	
Lorentzian	0.0001014501
Gaussian	0.0001100659
$4e^0$	0.00004
Lattice parameters	
a (Å)	10.5079735
b (Å)	5.6556616
c (Å)	12.0425029
beta(°)	113.5711
Volume(Å <sup>3</sup> )	715.6804345

#### 3.3 Thermal analysis

The thermal properties of the GLO crystal are studied using thermo gravimetric analysis (TGA) / differential thermal analysis (DTA) and differential scanning calorimetry (DSC). Powdered sample of 6.945 mg glycinium oxalate is analyzed in  $N_2$  atmosphere by using Perkin Elmer Diamond TGA / DTA equipment. The analysis is carried out simultaneously in air at a heating rate of  $10^\circ\text{C} / \text{min}$  for a temperature range of  $28^\circ\text{C}$  to  $810^\circ\text{C}$ . The TGA/DTA curve is shown in Fig. 3. Quite interesting and important point to be noticed is the very good thermal stability of the material up to  $190^\circ\text{C}$ . The absence of water of crystallization in the molecular structure is indicated by the absence of weight loss around  $100^\circ\text{C}$ . The endothermic peak in the DTA curve at  $179^\circ\text{C}$  represents the melting point of the sample. Another important observation is that there is no phase transition till the material melts and this aspect enhances the temperature range for the utility of the crystal for NLO applications. Further there is no decomposition up to the melting point. This ensures the suitability of the material for possible applications in lasers, where the crystals are required to withstand high temperatures. After  $190^\circ\text{C}$ , there is decomposition, illustrated by the loss of mass in the temperature range  $190^\circ\text{C}$  to  $240^\circ\text{C}$ . In this region the gaseous fragments like carbon dioxide and ammonia might be liberated.

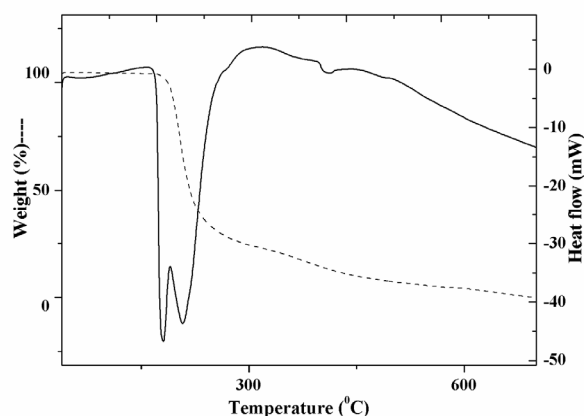


Fig. 3. TGA / DTA curve.

The DSC spectrum of the sample recorded with a Mettler Toledo DSC822 instruments with a heating rate of  $10^\circ\text{C}/\text{min}$  is shown in the Fig. 4. The endo thermic peak at  $179^\circ\text{C}$  corresponds to the melting point of the crystalline san

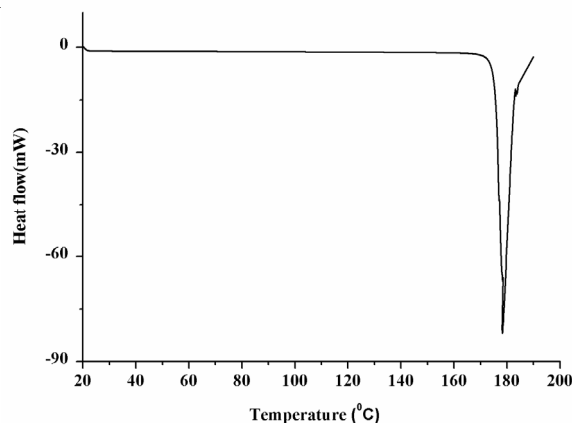


Fig.4. DSC curve.

### 3.4 UV-Vis-NIR spectrum

The transmission spectrum plays a vital role in identifying the potential of a NLO material because a given NLO material can be of utility only if it has a wide transparency window without any absorption at the fundamental and second harmonic wavelengths. The UV-Vis-NIR spectrum of the sample in the range 200nm-800nm is recorded with Hitachi U3140UV-VIS-NIR spectrophotometer and is shown in Fig. 5. It is evident that the crystal has a transparency window from 324nm to 800 nm making it suitable for applications in the whole region for higher harmonic generation. The absence of absorption of light in the visible region is an intrinsic property of all the amino acids [5].

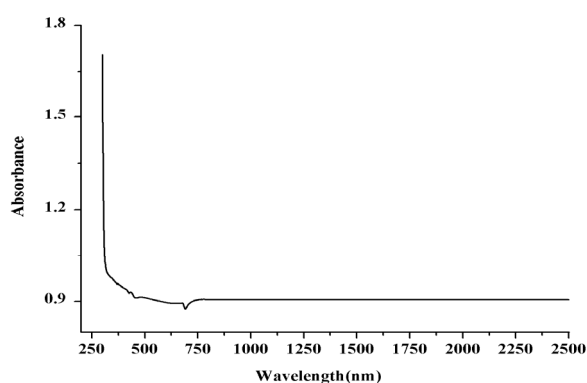


Fig.5. UV-Vis-NIR spectrum of GLO crystal.

### 3.5 FTIR analysis

The FTIR spectrum of the grown crystal is recorded using KBr pellet technique, in the wave number region  $500\text{ cm}^{-1}$  to  $4000\text{ cm}^{-1}$  using Thermo-Nicolate Avatar 370 system (Fig. 6).

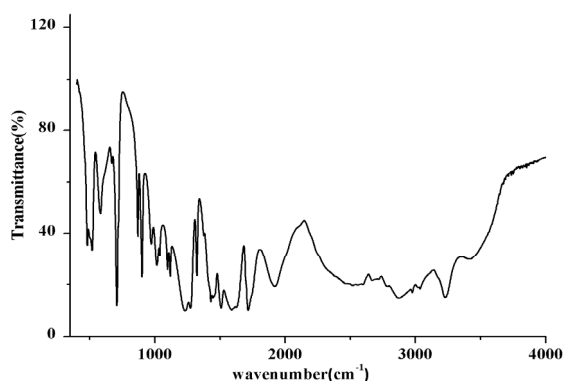


Fig.6. FTIR transmission spectrum.

Table 3. Vibrational assignments.

Peaks ( $\text{cm}^{-1}$ )	Assignment of vibrations
481	NH <sub>3</sub> + torsion mode.
518	COO rocking mode.
582	COO wagging mode / CH <sub>2</sub> out of plane bend
670	COO out of plane bending
708	COO in plane bending mode.
869	C- C stretching mode.
901	NH <sub>3</sub> rocking/CH <sub>2</sub> rocking in
972	NH <sub>3</sub> rocking
1015	O-H-Ostretching mode.
1037	CH <sub>2</sub> rocking out vibration.
1098	NH <sub>3</sub> + rocking mode.
1231	C-O stretch/O-H in plane bend
1322	CH <sub>2</sub> wagging vibration.
1429	CH <sub>2</sub> bending deformation.
1509	NH <sub>3</sub> + symmetric stretching mode.
1589	NH <sub>3</sub> + assymmetric deformation
1716	C=O stretching mode.
1922	C-C overtone
2873	O-H stretching
2974	CH <sub>2</sub> symmetric stretching mode.
3033	CH <sub>2</sub> assymmetric vibration
3229	NH <sub>3</sub> +assymmetric stretching mode.

Vibrational analysis of glycinium oxalate crystals is performed based on the vibrations of glycinium ion consisting of amino, methylene, carboxylic acid groups and oxalate ion. Observed bands are assigned on the basis of characteristic vibrations and are shown in table 3. The absorption peaks characterizing the various functional groups are in very good agreement with those reported in literature [6]. FTIR vibrational spectral analysis establishes the existence of NH<sub>3</sub><sup>+</sup> group in the crystal confirming the protonation of amino group for the formation of glycinium oxalate molecule.

### 3.6 Micro topography and etching studies

Good optical quality crystals free from defects are used for micro topographical studies using Leica Q Win Systems metallurgical microscope to check the presence of features like spirals, hillocks, slip lines...etc as they yield considerable have information about the growth mechanism [7]. We have observed two dimensional growth layers of small step height on the free surface of almost all the crystals (Fig. 7.a). Patterns like spirals, striations, slip bands, etc. are absent in the present study. The transmission photomicrograph of the inclusions present in the crystal is shown in Fig. 7 (b). A variety of parameters such as non-uniform growth rates, variation in super saturation during growth due to transition from dissolution to growth are responsible for these types of patterns. Kitamura et al. [8] pointed out that liquid

inclusions getting trapped parallel to the interfaces are due to drastic changes in growth conditions. GLO crystals show sharp cleavage on (010) plane, which shows river patterns and rivulets.

Chemical etching studies are carried out on the as grown and cleaved GLO crystals to study the symmetry of the crystal face from the shape of pits and the distribution of structural defects. First, the crystal is completely immersed in the etchant and then cleaned and dried and the etch figures are observed in the reflection mode. A mixture of n-propyl alcohol and distilled water is used as chemical polishing agent. Fig. 7 (c) shows the pyramidal hillock with a circle at the middle portion formed by etching with dilute propionic acid. When the surface dissolution is low, the surface is smooth and the increased dissolution at dislocations can lead to terracing (14). A composition of water in acetone in the ratio 1:5 volume is found to produce triangular etch pattern on the (010) surface when etched for 5-10 seconds is shown in Fig. 7 (d). When etched with water, fast dissolution layers are formed and are shown in figure 7.e. When etched with a mixture of acetic acid, methanol and distilled water circular etch pits are formed Fig. 7 (f). On successive etching no spurious development of pits is observed which suggests that etch pits are produced at the emergence of dislocation.

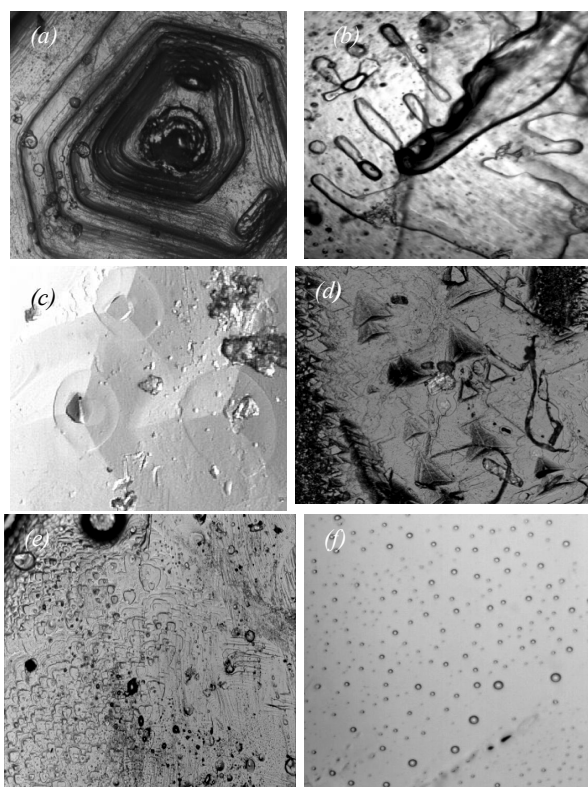


Fig.7. Microtopographical features of glycinium oxalate crystal. (a) layer pattern, (b) inclusions, (c) pyramidal etch hillock, (d) triangular etch pits, (e) fast dissolution layers, and (f) circular etch pits.

### 3.7 Photoconductivity studies

The GLO crystal is fixed on a glass plate and silver contacts are made over the sample to ensure good electrical contacts. It is then connected in series to a d. c. power supply and a Keithley 236 source measuring unit (picoammeter). Dark current and photocurrent by exposing the crystal to radiation from 100W halogen lamp for various applied electric fields are recorded and shown in Fig. 8. The photocurrent is found to be less than the dark current, which is termed as negative photoconductivity.

The phenomenon of negative photoconductivity is explained by Stockmann model [10]. The negative photoconductivity in a solid is due to the reduction in the number of charge carriers or their lifetime, in the presence of radiation [11]. For a negative photoconductor, forbidden gap contains two energy levels in which one is situated between the Fermi level and the conduction band while the other is located close to the valence band. The second state has higher capture cross-section for electrons and holes. As it captures electrons from the conduction band and holes from the valence band, the number of charge carriers in the conduction band gets reduced and the current decreases in the presence of radiation.

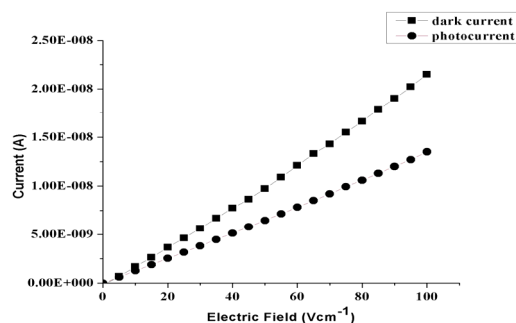


Fig.8. Field dependence of photo and dark current.

### 3.8 Photo-luminescence studies

Photo-luminescence spectrum is recorded with a Jobin Yvon Spectrofluorometer (Model FL3-22). A 450 W xenon lamp is used as the source and PMT (Model R928P) as the detector. Double gratings are used for the excitation and emission spectrometers. The excitation wavelength used for the present study is 320 nm and the spectrum recorded is shown in Fig. 9. It is broad, comprising green to ultraviolet emission in the 1.75-3.60 eV range in which the maximum intensity is observed at 470 nm and then the intensity is slowly reduced in the higher wavelength region. Another strong peak at 564 nm is also observed.

The main contribution to the HOMO state comes from the COO<sup>-</sup> ions, while to the LUMO state comes from the NH<sub>3</sub><sup>+</sup> ions. In amino acid molecular chains, these two molecular orbitals are at opposite extrema. So, in the interband transitions, the electron has to cross the whole chain, losing energy to the vibrational modes of the crystal, contributing to the luminescence [12]. Peaks in the visible region can be assigned to lattice related

processes, while the peaks in the UV region can be due to the relaxation of excited molecular states.

The maximum intensity peak at 470nm is due to the protonation of amino group to the carboxyl group. The lowering of photoluminescence intensity at higher wavelength region may be attributed to a relatively low barrier for rotation of the carboxyl group around the central C-C bond [13].

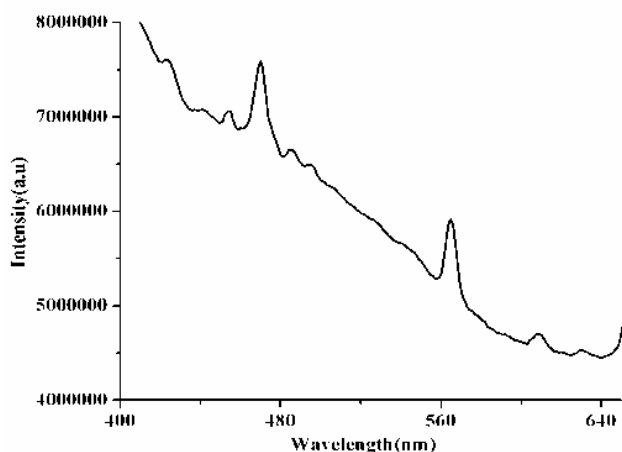


Fig. 9. Photo-luminescence spectrum of GLO.

### 3.9 Z scan studies

The non-linear optical properties and the optical limiting performance of this compound are investigated using Z scan technique, for which 532nm laser pulses of 8ns duration and 128  $\mu\text{J}$  are used. The experimental data taken under an open aperture is plotted in figure 10 which clearly illustrates that the absorption increases as the incident light irradiance increases and that the light transmittance (T) is a function of the sample's Z position (with reference to the focal point at Z = 0). Fig. 11 shows transmission minimum at the focal point, which is a clear indication of nonlinear two-photon absorption. There is also very good agreement between the experimental data and the theoretical fit. The NLO absorption data obtained under the conditions used in this study can be well described by equations (1) and (2) [14, 15] where  $\alpha$  and  $\beta$  are the linear and effective third order NLO absorptive indexes respectively,  $\tau$  is the time, and L is the optical path length.

$$T(z) = \frac{1}{\sqrt{2\pi}} \int_{-\infty}^{\infty} \ln[1 + Q(\tau)] e^{-\tau^2} d\tau \quad (1)$$

$$Q(z) = \beta I(z) \frac{1 - e^{-\alpha L}}{\alpha} \quad (2)$$

The effective nonlinear absorptive index  $\beta$  is measured to be  $2.583 \times 10^{-10} \text{ mW}^{-1}$ . The comparatively high value of two photon absorptive index demonstrates that the GLO crystal has potential for optical limiting applications.

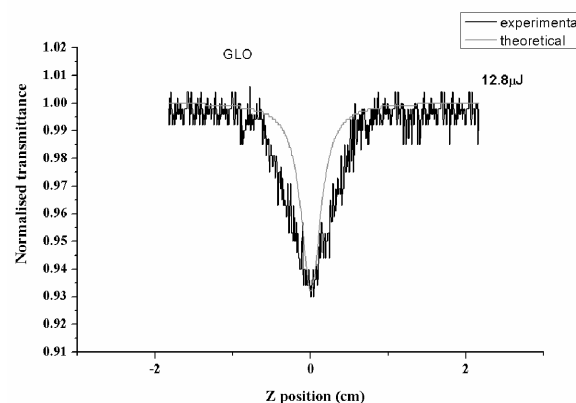


Fig. 10. Z scan spectrum under open aperture configuration.

## 4. Conclusions

The charge transfer complex crystal of amino acid glycine and oxalic acid – Glycinium oxalate is successfully grown in bulk size using top seeded solution growth method at room temperature and characterized by powder XRD and CHN analysis. Micro topographical and etching study reveals that crystal growth mechanism is by 2D nucleation and subsequent spreading of layers. Thermal studies show that the material is thermally stable without any phase transition up to the melting point (179°C). Since there is no decomposition observed up to 190°C, crystallization can be done by melt method too. FTIR studies confirm the various functional groups and their vibrational interactions. UV-Vis-NIR studies show that the crystal has a wide transparency window from 324 nm to 2500 nm enables it to be a good candidate for optoelectronic applications. Photoconductivity studies establish that GLO crystal is a negative photoconductor. Open aperture Z scan analysis suggests that GLO crystals can be used for optical limiting applications.

## Acknowledgements

The authors would like to acknowledge with thanks the co operation extended by Dr. M.K. Jayaraj, Reader, and Miss. R. Sreeja, Research scholar, Department of Physics, CUSAT, Kerala, India for taking the Z scan measurements.

## References

- [1] W. A.Schoonweld, J. Wildeman, D. Fichou, Nature **404**, 977(2000)
- [2] J. Zyss, J. F. Nicoud, Curr. Opin. Solid State Mater. Sci. **1**, 533 (1996).
- [3] M. Subhanadinini, R. V. Krishnakumar, S. Natarajan, Acta. Cryst. **C57**, 165 (2001).

- [4] G. S. Pawley, *J. Appl. Cryst* **14**, 357(1981).
- [5] R. Silverstein, G. C. Bassler, *Spectrometric identification of organic compounds*, John Wiley & sons, New York, (1981).
- [6] D. Sajan, J. Binoy, B. Pradeep, *Spectrochem. Acta* **A60**, 173(2004).
- [7] M. S. Joshy, A. S. Vagh, *Ind. J. Pure & Appl. Phys.*, **5**, 318(1967).
- [8] M. Kitamura, A. Kouchi, *J. Miner.* **3**, 119 (1982).
- [9] K. Sangwal, *Etching of crystals*, North Holland Physics Publication, Amsterdam, (1987).
- [10] V. N Joshi, *Photoconductivity*, Marcel Dekker, New York, (1990).
- [11] R. H. Bube, *Photoconductivity of solids*, Wiley, New York, (1981).
- [12] E. W. S. Caetano, J. R. Pinheiro, M. Zimmer, V. N. Frierie, G.A.Farias, *AIP conf. Proc.* **772**, 1095 (2005).
- [13] A. Aravindan, P. Srinivasan, *Crystal Res. Technol.* **11**, 1097 (2007)
- [14] M. Sheik Bahae, A. A. Said, H. Wei, D. J. Hagan, *IEEE J. Quantum. Electron.* **26**, 760 (1990).

\*Corresponding author: arun\_k\_j@yahoo.co.in